JOURNAL OF MATERIALS SCIENCE 26 (1991) 4196–4202

Studies on carbon fibre reinforced aluminium composite processed using pre-treated carbon fibres

S. N. PATANKAR*, V. GOPINATHAN, P. RAMAKRISHNAN
Department of Metallurgical Engineering, Indian Institute of Technology, Bombay 400 076, India

Carbon fibre reinforced Al-12% Si alloy composite has been fabricated by pre-treating the fibres with K_2ZrF_6 followed by molten alloy infiltration and subsequent hot pressing of the preforms. The infiltration conditions were arrived at based on the measurement of tensile strength of the fibres extracted from the preforms. The fibre volume per cent of 20 was found to result in composite tensile strength of about 240 MPa as compared to tensile strength of 100 MPa for the unreinforced matrix. Characterization of the interface revealed the formation of $ZrSi_2$ and diffusion of potassium and aluminium into the fibre. The interfacial bonding was strong as is evinced by the absence of fibre pull-out on to the fracture surface.

1. Introduction

The widespread acceptance of carbon fibre reinforced aluminium composite for structural applications has been limited due to the various problems encountered during the fabrication of the composite, foremost among them being poor wettability of carbon with aluminium. A good wettability is essential to ensure impregnation of individual fibre in the tow by molten aluminium. Methods of fabricating these composites therefore have generally involved the use of techniques such as thermo-vacuum treatment of the fibres, metallic and ceramic coating on the fibres, suitable alloying addition to aluminium, etc. in order to achieve good wetting during infiltration [1–4]. More recent and entirely different approach to overcome the problem of wetting in C/Al composites is by pre-treatment of the carbon fibre with K_2ZrF_6 [5, 6]. Present work deals with characterization of the C/Al composite fabricated by K_2ZrF_6 pre-treatment route.

2. Experimental procedure

2.1. Fabrication of the C/Al composite

Torayca T300–3000 carbon fibres were used in the present investigation. The organic sizing layer present on the as-received carbon fibres was removed by treating the fibres with acetone. The removal of the sizing was ascertained using Fourier transform infrared spectroscopy in attenuated total reflectance (ATR) mode. These fibres were then treated with K_2ZrF_6 and dried in vacuum at 100 °C. The preforms were made by infiltration of molten alloy of Al-12 wt % Si. To optimize the infiltration conditions, several infiltration tests were carried out using an infiltration (contact) time of five seconds and melt temperature varying from 600 to 800 °C. The carbon fibres were subsequently extracted by dissolving away the matrix using sodium hydroxide. The extracted fibres were dried, separated and subjected to single fibre tensile testing. Thirty fibres were tested corresponding to each infiltration temperature and mean tensile strength estimated using Weibull statistical distribution. Table I shows the variation of mean tensile strength with infiltration temperature. There is a steady decrease in the tensile strength value with increasing melt temperature. A temperature of 650 °C was chosen for the present experimental investigation as it represents a reasonable compromise from considerations of melt fluidity and fibre damage. Similar infiltration experiments were performed to optimize the contact time of carbon fibres with molten aluminium. Contact time of five seconds was the minimum required to be maintained during the actual infiltration. Higher contact times at 650 °C led to the progressive deterioration in the fibre strengths as is evident from Table II which shows the effect of contact time on the fibre strength. The preforms were hot pressed at 500 °C using a compaction pressure of 150 MPa for two minutes to form the final composite samples.

2.2. Characterization of C/Al composite

Specimens for transmission electron microscopy (TEM) observations were prepared by cutting thin cross-sections of the C/Al composite using a diamond

* *Present address*: Department of Metallurgy and Materials Engineering, New Mexico Tech, Socorro, NM 87801.

0022–2461/91 $03.00 + .12

TABLE I Effect of infiltration temperature on the Weibull mean tensile strength of the carbon fibres

Infiltration temperature (°C)	Scale parameter α	Shape parameter β	Weibull mean tensile strength (MPa)	Standard deviation	Coefficient of variation (%)
600	0.75×10^{-15}	4.03	3401	955.06	28.08
650	0.43×10^{-27}	7.92	2678	397.9	14.8
700	0.10×10^{-9}	2.95	2158	808.43	37.46
750	0.25×10^{-18}	5.60	1942	404.29	20.81
800	0.24×10^{-15}	4.90	1516	327.38	21.59

TABLE II Effect of contact time during infiltration on the Weibull mean tensile strength of carbon fibres

Infiltration time (s)	Scale parameter α	Shape parameter β	Weibull mean tensile strength (MPa)	Standard deviation	Coefficient of variation (%)
5	0.43×10^{-27}	7.92	2678	397.9	14.8
15	0.21×10^{-15}	4.74	1829	444.3	24.29
30	0.27×10^{-12}	3.85	1635	482.72	29.52
45	0.32×10^{-14}	4.49	1531	393.2	25.68
60	0.56×10^{-19}	6.01	1474	284.55	19.3
75	0.25×10^{-15}	4.88	1430	337.98	23.63

saw. These sections were then mechanically polished to 100 μm thickness, dimpled and further thinned by argon ion bombardment. The ion-milled specimens were observed in 300 keV analytical transmission electron microscope. Scanning electron microscopic technique, utilizing an instrument equipped with electron probe micro-analyzer (EPMA) was used for analysis of fracture surfaces and for microstructural analysis of the composite specimen. Specimens were prepared for fractographic studies by cutting the fracture end from the composite bar and ultrasonically cleaning the fracture end in acetone. C/Al composite specimens were also mounted and polished for microstructural examination by SEM. The ESCA experiments were performed on the carbon fibres extracted from aluminium matrix in a commercial photoelectron spectrometer.

3. Results and discussion

Fig. 1 shows the optical photomicrograph of cross-section of carbon fibre reinforced aluminium composite. It is apparent from this micrograph that there is satisfactory infiltration of molten aluminium in the tow. The fibre–matrix interface is smooth with no discontinuities observed even at higher magnification as is exemplified by Figs 2 and 3 which are scanning electron micrographs of C/Al composite. However,

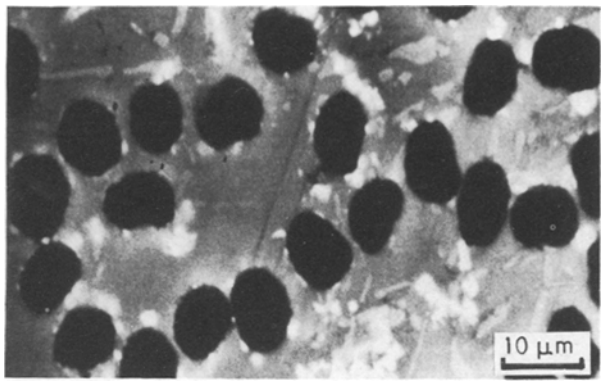

Figure 2 Scanning electron micrograph of carbon fibre/aluminium composite showing the presence of reaction products both in the bulk as well as in the interfacial region.

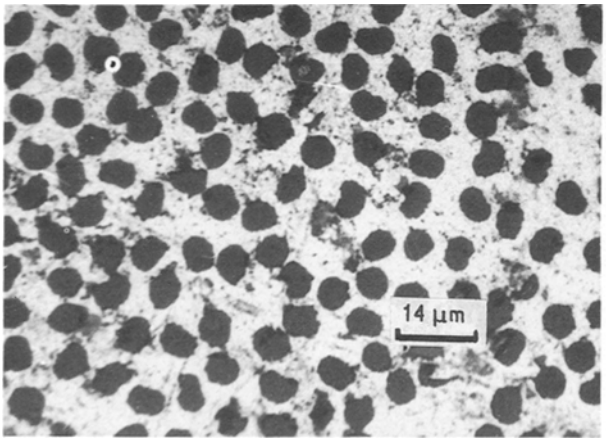

Figure 1 Optical micrograph of carbon fibre/aluminium composite. The distribution of the fibres in the composite appears to be fairly uniform.

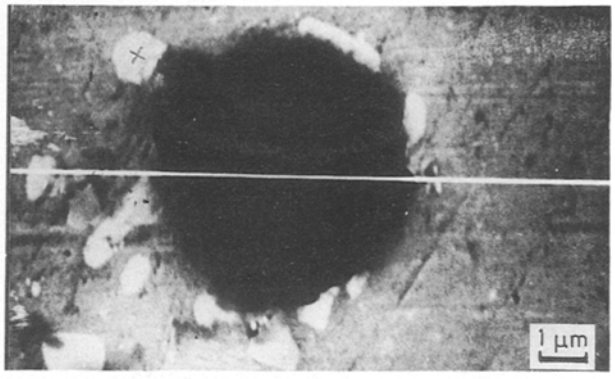

Figure 3 Scanning electron micrograph of carbon fibre/aluminium composite. The electron probe micro-analysis of the region marked '×' revealed that the reaction product was a Zr-Si intermetallic with the empirical formula of the type $ZrSi_2$.

these micrographs show the presence of certain reaction product both in the bulk as well around fibre–matrix interface. The reaction product is probably the outcome of reaction between the K_2ZrF_6 treated carbon fibre and the aluminium matrix.

With the introduction of 20 vol % of fibres in the matrix there was an increase in the tensile strength from 109 MPa to 240 MPa. The fracture surfaces of the C/Al composite were examined to determine the nature of the composite failure. Figs 4 and 5 show the SEM fractographs taken with 0° and 50° tilt angles, respectively. From these micrographs the fracture appears almost coplanar. There is no indication of any fibre pullout because even the SEM fractograph taken with tilt angle as high as 50° fails to show appearance of any protruding fibre. The failure seems to be through the matrix and not occurring at the interface. In the present case the fibre is brittle and the matrix being 12.4% silicon aluminium alloy has limited ductility. The fracture of the fibre embedded in the matrix of this type cause the matrix adjacent to fibre break to be loaded rapidly and the sudden release of stored energy in the fibre is available to allow the fibre crack to propagate into the matrix. In the composites with strong fibre–matrix interface as in the present case, the fibres ahead of the advancing crack front are broken and the remaining bridges of the matrix then neck down in a completely ductile manner.

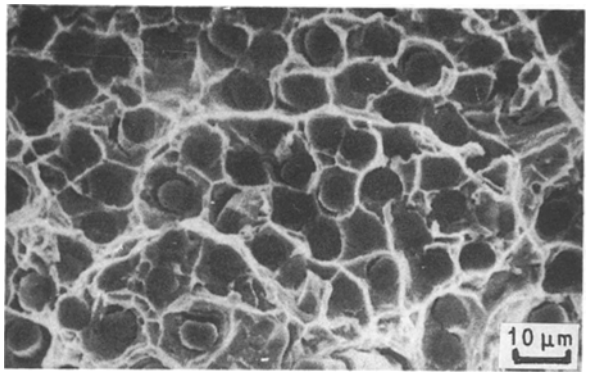

Figure 4 SEM fractograph (0° tilt) of carbon fibre/aluminium composite showing planar fracture surface.

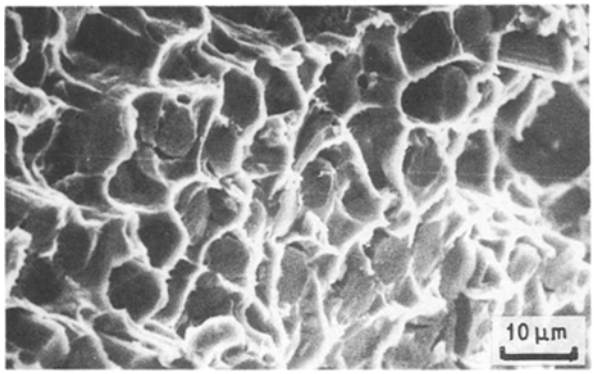

Figure 5 SEM fractograph (50° tilt) of carbon fibre/aluminium composite fails to show evidence of any fibre pull-out.

3.1. Electron probe micro-analysis

Figs 6 and 7 show, respectively, the elemental distribution of silicon and zirconium in the C/Al composite. Zirconium distribution appears to be non-uniform. Silicon distribution shows the presence of silicon rich needles in the matrix. The common patches in the silicon and zirconium elemental distribution suggests the existence of zirconium-silicon intermetallic. In metal matrix composites the enrichment of the alloying elements occurs in the interfacial region. In the case of carbon fibre aluminium composite the alloying elements are rejected from the matrix material during the reaction between the fibre and the matrix that leads to the formation of Al_4C_3. These rejected elements accumulate at the interface [7, 8]. This explains the segregation of silicon seen in the EPMA line scan, taken across the C/Al interface, Fig. 8. The segregation of Zr, also observed across the C/Al interface could be due to the formation of intermetallics (e.g. aluminides or silicides of Zr).

The elemental analysis results corresponding to point marked '×' in Fig. 3 obtained using EPMA are shown in Table III. The atomic percentage ratio of zirconium to silicon is found to be 1:2. This indicates

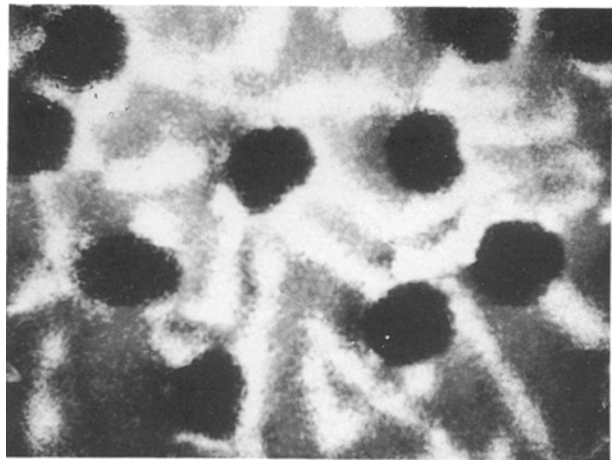

Figure 6 X-ray map of silicon showing distinct appearance of characteristic silicon rich needles in carbon fibre/aluminium composite.

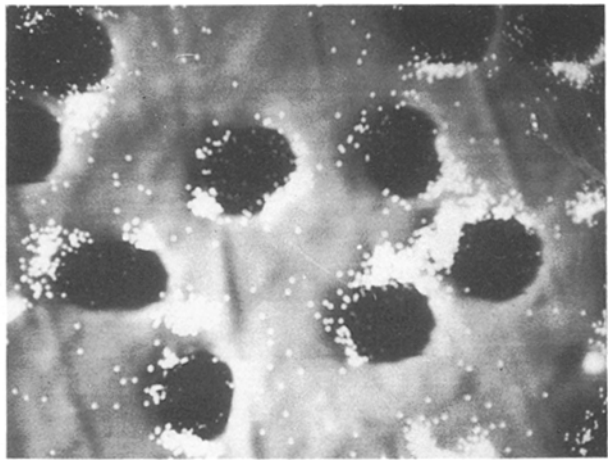

Figure 7 X-ray map of zirconium showing non-homogenous distribution of zirconium in carbon fibre/aluminium composite.

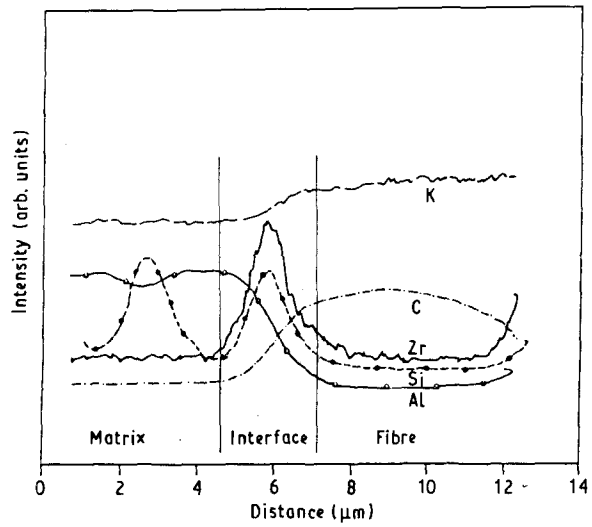

Figure 8 EPMA line scan of Al, Zr, C, Si and K across C (fibre)/Al interface.

TABLE III Electron probe micro-analysis of carbon fibre reinforced aluminium composite

Elemental analysis (% atomic concentration)			Ratio of % atomic concentrations	Predicted compound
Al	Si	Zr	Si/Zr	
10.23	58.79	30.89	1.9	$ZrSi_2$

that precipitate seen in Fig. 3 at point marked '×' is a compound with empirical formula of the type $ZrSi_2$.

3.2. Electron spectroscopy for chemical analysis

Table IV shows the binding energy of Zr 3d and O 1s electrons (obtained from their X-ray photoemission spectra shown in Figs 9 and 10, respectively). These data were obtained from the photoemission spectra of the carbon fibres extracted from C/Al composite. The spectra of Zr 3d region consist of $3d_{5/2}$ and $3d_{3/2}$ doublet as can be seen in Fig. 9. Zr $3d_{5/2}$ peak occurs at 178.0 eV when Zr is in the free state (zero valency) [9]. However, when Zr is present in combined form as ZrO_2 the same peak would occur at 182.2 eV [10]. In the present case the Zr $3d_{5/2}$ peak was found at 182.2 eV strongly suggesting the presence of ZrO_2 on the carbon fibres extracted from the C/Al composite.

Rocher *et al.* [5] suggested that depending on the composition of the matrix, K_2ZrF_6 reacts with aluminium matrix leading to the formation of either $ZrAl_3$ or $ZrSi_2$ as represented by the following reactions

$$3K_2ZrF_6 + 4Al \rightarrow 4AlF_3 + 6KF + 3Zr$$

$$Zr + 3Al \rightarrow ZrAl_3 \text{ (When the matrix is pure Al)}$$

$$Zr + 2Si \rightarrow ZrSi_2 \text{ (When the matrix is Al-Si alloy)}$$

TABLE IV Binding energy values of Zr 3d and O 1s obtained from XPS spectra of carbon fibres extracted from C/Al composite

	Binding energy (eV)	Probable compound
Zr $3d_{5/2}$	182.2	Oxide (ZrO_2)
O 1s	530.7	Oxide (ZrO_2)

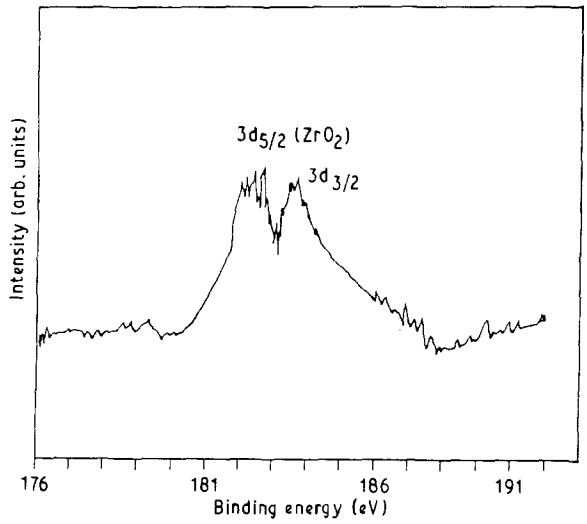

Figure 9 Zr 3d photoemission spectra of carbon fibres extracted from C/Al composite.

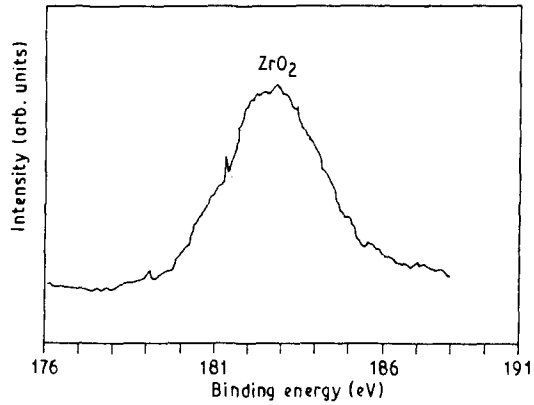

Figure 10 O 1s photoemission spectra of carbon fibres extracted from C/Al composite.

Thus in the C/Al composite fabricated by K_2ZrF_6 route either of the two compounds $ZrAl_3$ (when the matrix is pure Al) or $ZrSi_2$ (when the matrix is Al-Si alloy) is expected to be present at the carbon fibre aluminium matrix interface. In any case when the carbon fibres are extracted from the C/Al composite by dissolving the matrix using NaOH, ZrO_2 would be formed on the surface of the extracted fibres as explained below.

When Al-Zr intermetallic compound ($ZrAl_3$ for example) comes in contact with NaOH then the Al part of the compound on account of its amphoteric nature will dissolve in NaOH leaving behind elemental Zr. The elemental Zr has a tendency to undergo oxidation to form ZrO_2

$$2ZrAl_3 + 6NaOH + 6H_2O \rightarrow 6NaAlO_2 + 2Zr + 9H_2$$

$$Zr + O_2 \rightarrow ZrO_2$$

Similarly when Al-Si intermetallic compound(silicide) reacts with NaOH there is hydroxide formation as suggested by the following general chemical equation

$$M_2Si + 4H_2O \rightarrow 2M(OH)_2 + SiH_4$$

This is one of the standard methods of preparation of

silane(SiH_4). The hydroxide formed subsequently decomposes leaving behind corresponding oxide

$$Zr(OH)_4 \rightarrow ZrO_2 + 2H_2O$$

Latter is the plausible explanation for the occurrence of ZrO_2 on to the extracted carbon fibres (as detected by ESCA) in the present study.

3.3. Transmission electron microscopy (TEM)

Fig. 11 is a TEM bright field image of the transverse section of the C/Al composite. It appears from this figure that the C/Al interface is not just a sharp demarcation line between carbon fibre and aluminium matrix, but is a diffused region comprising of acicular crystals grown in the direction transverse to the axis of the fibre. These fine structures appear more prominent in Fig. 12. The EDAX pattern taken at point marked '×' in Fig. 13 showed the presence of aluminium, silicon and zirconium. Similar acicular shaped crystals of Al_4C_3 have been reported to be formed by Blankenburg [11] in case of C/Al composite. The presence of Al_4C_3 crystals in these crystallites could be ascertained using highly sophisticated characterization techniques. Fig. 13 is also a TEM picture of the C/Al interfacial region showing the presence of a reaction product in the form of precipitate particle. The EDAX pattern taken at point marked '×' on to the precipitate particle indicated that it chiefly comprised of silicon and zirconium. To identify the precipitate particle an electron diffraction pattern (EDP) was taken at point marked '×' on the particle and is shown in Fig. 14. The interpretation of this EDP revealed the fact that the precipitate particle found near the C/Al interface was that of $ZrSi_2$. Fig. 15 shows the schematic of the duly labelled EDP.

Apart from the reaction zone, the C/Al interface also consists of a diffusion zone in the fibre along the periphery. Fig. 16 is a TEM picture of C/Al interface showing such a region. In this figure at point marked '×' in the inner side of the fibre the EDAX pattern showed the presence of potassium and aluminium. The existence of potassium in the carbon fibre suggests the formation of intercalation compounds resulting from the insertion of potassium ion in between the basal layers of carbon fibre structure. The formation of such intercalation compounds probably induce wetting of the carbon fibre by molten aluminium.

Chemical interaction at C/Al interface could be discussed in the light of the TEM results as follows: Carbon and aluminium react above 450 °C to form Al_4C_3 [12]. In C/Al composite system the reaction determining the bond strength between carbon fibre and aluminium matrix is the one that leads to the formation of Al_4C_3. The carbide phase grows as acicular inclusions which embed themselves both in the fibres and in the matrix, thereby forming local

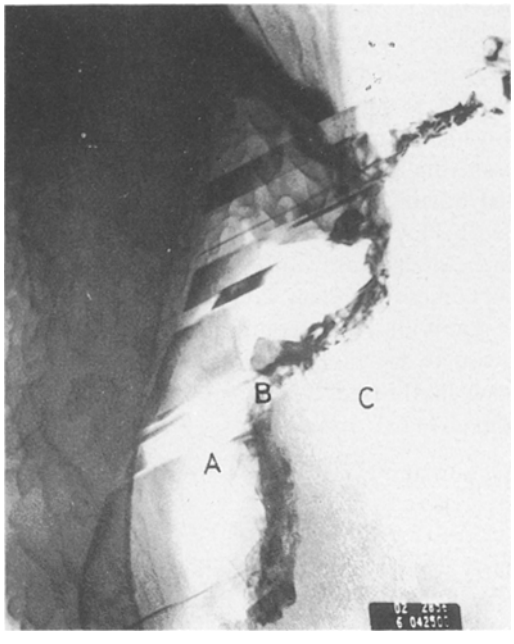

Figure 11 TEM picture of C/Al interface. (A) matrix, (B) interface and (C) fibre (Magnification 42500×). The C fibre Al interface appears to be made up of colonies of crystallites.

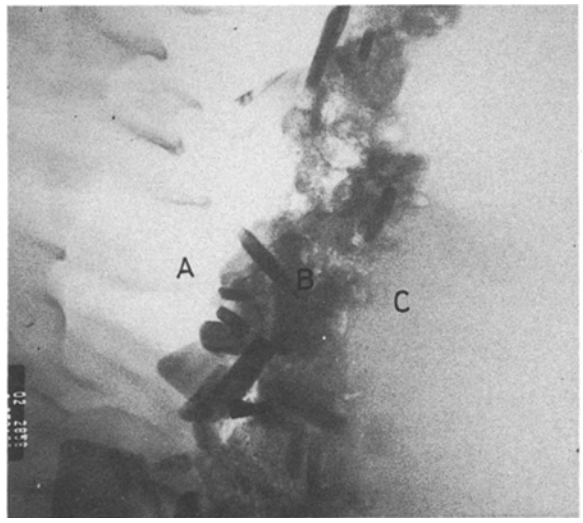

Figure 12 TEM picture of C/Al interface. (A) matrix, (B) interface and (C) fibre (Magnification 52100×). The colonies of crystallites formed at the C/Al interface due to the interaction of K_2ZrF_6 treated C fibres with Al matrix are clearly visible.

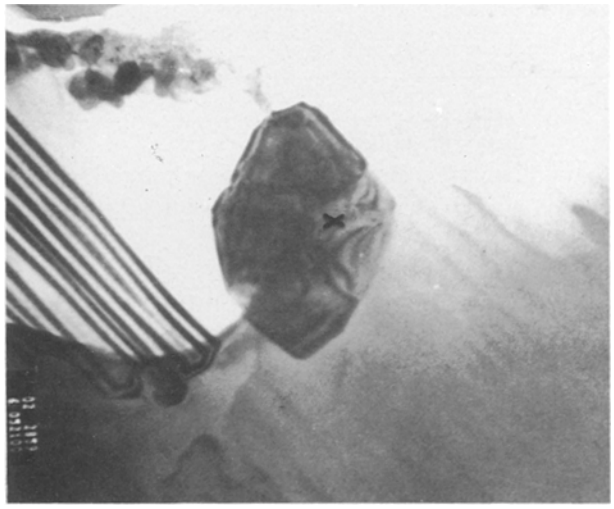

Figure 13 TEM picture of C/Al interface. (Magnification 52100×). The precipitate particle seen in the C/Al interfacial region is a Zr-Si intermetallic (as indicated by EDAX).

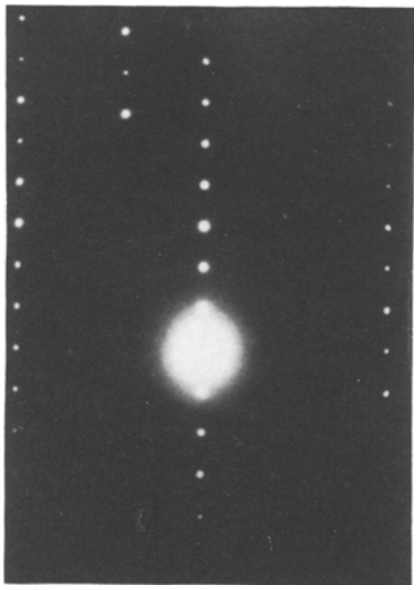

Figure 14 Electron diffraction pattern taken at region marked '×' in Fig. 13.

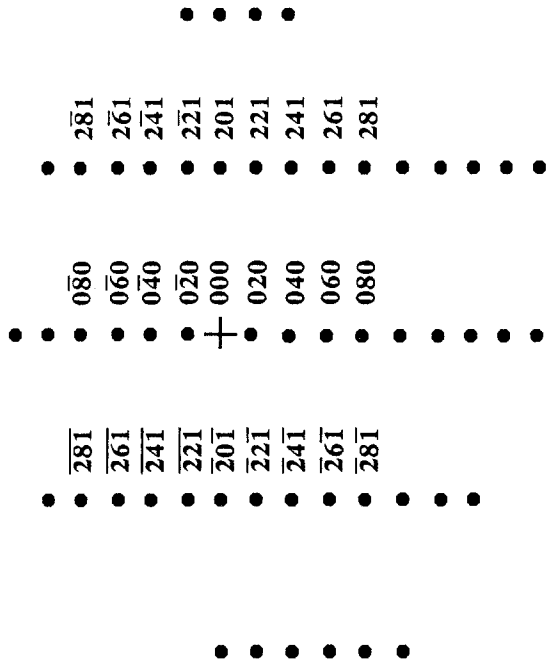

Figure 15 Schematic of the labelled electron diffraction pattern.

bond sites. Carbides nucleate individually on the surface of fibre and increase in size with time and rise in temperature. Non-uniform nucleation results in the formation of colonies of carbides. In the present case the K_2ZrF_6 crystals present on the fibre surface react with the Si of Al-Si alloy (which is the matrix material) resulting in the formation of $ZrSi_2$. The silicide formation causes localized heating thereby raising the temperature for carbide formation. Thus application of K_2ZrF_6 creates conditions which are conducive for carbide formation during liquid metal infiltration. Each crystal of K_2ZrF_6 present on the fibre surface serves as a nucleating centre for carbide crystal formation. Large numbers of these carbide crystals or the cohesion bridges strengthen the fibre–matrix bond.

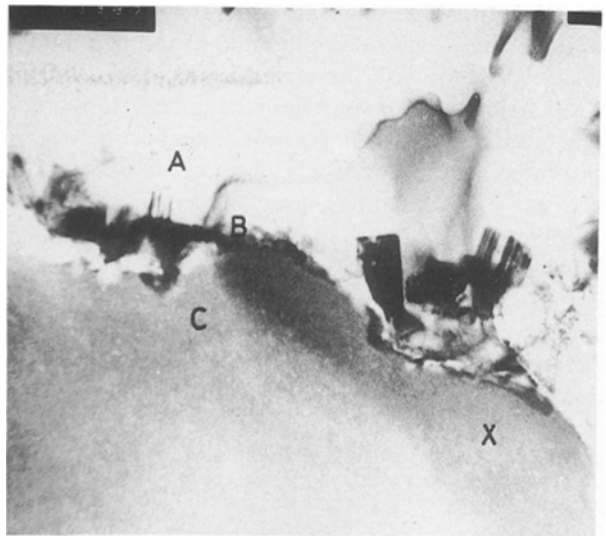

Figure 16 TEM picture of C/Al interface. (A) matrix, (B) interface and (C) fibre (Magnification 50000×). EDAX pattern taken at region marked '×' in the C fibre indicated the existence of diffused Al and K.

Too strong a fibre–matrix bond does not allow the energy absorbing mechanisms like fibre pull-out to operate in the interfacial region. Hence the composite fracture surface is expected to be planar without any indication of fibre pull-out, as in the present case.

Because of the incompatibility between carbon fibre and aluminium matrix by the virtue of difference in their thermal expansion coefficients, the C/Al interface is expected to serve as sink for the dislocations. Fig. 17 which is a TEM picture of C/Al interface shows such pile-up of dislocations near the carbon fibre aluminium interface.

4. Conclusion

The pre-treatment of the carbon fibres with K_2ZrF_6 resulted in improved fibre wetting characteristics and

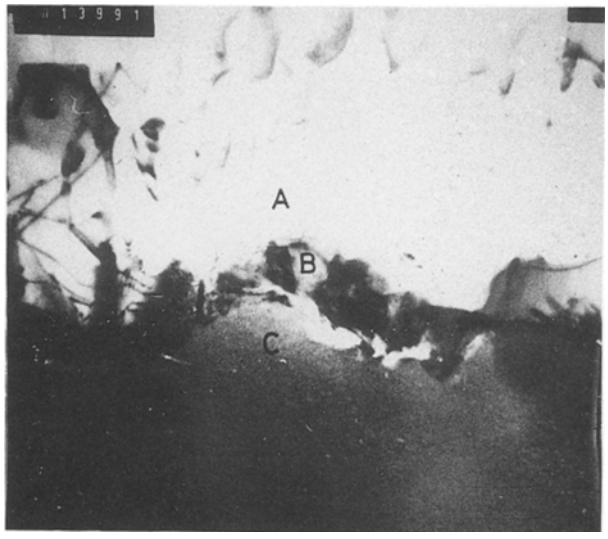

Figure 17 TEM picture of C/Al interface. (A) matrix, (B) interface and (C) fibre (Magnification 50000×). Dislocation pile-up in the interfacial region appears due to the difference in the thermal expansion coefficient of carbon fibre and aluminium matrix.

good matrix–fibre interfacial bonding in the composite. There was a nominal improvement in the tensile strength with the introduction of the fibres in comparison with the unreinforced matrix. In the current study the carbon fibres were treated with aqueous saturated solution of K_2ZrF_6 because of which there was no precise control over the crystallization of K_2ZrF_6 on to the fibre surface and on the subsequent fibre–matrix interfacial reaction leading to the fibre damage. With the proper choice of the solvent however, even low concentration of K_2ZrF_6 can cause effective wetting of carbon fibres with minimum fibre damage.

Acknowledgement

Authors wish to thank Dr Deepankar Banerjee, Dy. Director, Defence Metallurgical Research Laboratory, Hyderabad, India for providing the TEM facilities.

References

1. A. A. BAKER, A. MARTIN and R. J. BACHE, *Composites* **2** (1971) 154.
2. A. KIMURA, T. TERAOKA and R. SAGARA, in 'Proceedings of the 4th International Conference on Composite Materials', Japan, 1982, edited by T. Hayashi, K. Kawa and S. Umekawa, p. 1451.
3. M. S. RASHID and C. D. WIRKUS, *Ceramic Bulletin* **51** (1972) 836.
4. O. A. KASHIN and A. A. ZABOLOTSKII, *Metal Sci. and Heat Treatment* **22** (1982) 809.
5. J. P. ROCHER, J. M. QUENISSET and R. NASLAIN, *J. Mater. Sci. Lett.* **4** (1985) 1527.
6. *Idem., J. Mater. Sci.* **24** (1989) 2697.
7. J. C. VIALA, F. BOSSELET, P. FORTIER and J. BOUIX, in Proceedings of the 6th International Conference on Composite Materials, London, 1987, edited by F. L. Mathews, F. L. Buskell, N. C. R. Hodgkinson and J. Morton, p. 146.
8. T. ERTURK, V. GUPTA, A. S. ARGON and J. A. CORNIE, in *ibid.* p. 156.
9. L. RAMQVIST, *J. Phys. Chem.* **30** (1969) 1835.
10. K. HORN, S. KRAUSE and G. WEINBERG, *Thin Solid Films* **150** (1987) 41.
11. G. BLANKENBERG, *J. Australian Institute of Metals* **14** (1969) 236.
12. B. MARUYAMA and L. RABENBERG, in Proceedings of the Symposium sponsored by AIME-AMS, Louisiana, 1986, edited by A. K. Dhingra and S. G. Fishman, p. 233.

Received 13 March
and accepted 3 December 1990